Catalysis Letters 3 (1989) 143–158

A CATALYTIC STUDY OF FORMIC ACID OXIDATION ON PREFERENTIALLY ORIENTED PLATINUM ELECTRODES

L. PALAIKIS and A. WIECKOWSKI

Department of Chemistry, University of Illinois, 1209 W. California St., Urbana, Illinois 61801, U.S.A.

Received 6 April 1989; accepted 20 June 1989

Formic acid oxidation, platinum electrocatalysis

The oxidation of formic acid was examined by cyclic voltammetry and chronoamperometry in order to determine the rate of catalytic activity (reaction turnover) as a function of surface crystallography on preferentially oriented (electrochemically modified) platinum electrodes. The resulting turnover rates indicated a maximum fourfold current enhancement for an approximately 60% (111)-oriented surface versus a polycrystalline surface, suggesting that preferentially oriented electrodes are of potential practical significance.

1. Introduction

The study of the catalytic oxidation of formic acid has been active over the last three decades and a number of comprehensive reviews indicating the practical importance of this process have been published [1–6]. The oxidation of formic acid shows pronounced structure sensitivity at low index metal surfaces [7–13]. However, the use of single crystals in real-life electrocatalytic applications is impractical due to their high manufacturing costs. More recently, a procedure for the preparation of preferentially oriented surfaces that approximate the characteristics of single crystals has been pioneered by Arvia et al. [14–17]. The objective of this work was to assess the influence of surface crystallography on the rate of formic acid oxidation at such preferentially oriented Pt surfaces.

2. Experimental details

Oxygen-free nitrogen (Linde), reagent grade formic acid (Fischer) and reagent grade sulfuric and perchloric acids (Fischer) were used in this study. All electrochemistry experiments (orientation, voltammetry, and chronoamperometry) were

carried out using a three-compartment glass cell equipped with a Luggin capillary. All potentials are given with respect to Ag/AgCl, $[Cl^-] = 1.0$ M NaCl. The working electrode was a 1 mm diameter round platinum wire (Johnson Matthey, purity = 99.95%), the prepared working face (geometric area = 0.785 mm^2) contacting the solutions via a meniscus arrangement. The small area electrode was chosen to minimize the capacitive component of the current passes, thus reducing the cell time constant, $R_u C_d$, and preventing significant lag in the potential at the working interface. The working surface was prepared by polishing with diamond past down to 0.25 μm, degreasing in warm sulfuric acid, soaking in concentrated hydrofluoric acid to remove any carbonaceous residue, and hydrogen annealing followed by quenching. A final step in the preparation involved electrochemically stepping the surface between the O_2 and H_2 evolution threshold potential limits to remove any remaining surface impurities. Cyclic voltammetry was used as a check for surface cleanliness.

In preparing the preferentially oriented surfaces the working electrode was immersed ~ 2 mm into 0.5 M H_2SO_4 electrolyte, chosen for its voltammetric enhancement of the hydrogen adsorption-desorption peaks used in assessing the degree of orientation achieved. Electrochemical orientation involves the selective redistribution of a polycrystalline surface to a desired crystallographic orientation by applying a fast periodic square wave potential perturbation between the potential limits characterizing the underpotential decomposition of water [14–17]. The square wave potential perturbation was applied with the signal generated using a function generator (Dynascan Model 310), fed into the external input of the potentiostat (PAR model 273) and monitored using an oscilloscope. The (100) orientation parameters were: lower potential (E_l) = −0.15 V, upper potential (E_u) = 1.2 V, frequency (f) = 2.5 kHz, time = 10 hours. The (111) orientation parameters were: (E_l) = 0.50 V, (E_u) = 1.20 V, (f) = 2.0 kHz, time = 2.5 hours.

Scanning electron micrographs and corresponding electron channeling (backscatter) patterns were obtained using a JEOL model JSM-35C scanning electron microscope modified for channeling applications. In obtaining the backscatter patterns, an ~ 30 μm disc of least confusion (spot size) was utilized.

Chronoamperometric data were collected for 0.1 M formic acid in 0.5 M perchloric acid (chosen for its non-affinity towards platinum). A prestep from 0.0 V to 1.2 V was initiated to ensure a clean starting surface free of any adsorbed species or poisons. A potential step from 1.2 V to an intermediate potential in the range covering the double-layer and species oxidation threshold region (0.10 V to 0.45 V) was then applied in order to monitor the steady-state kinetics of formic acid electrooxidation. The duration of the potential program was determined by the time needed for the current to decay to negligible values after reaching the intermediate potential. The current response of the electrolyte was subtracted point-by-point from the current values of the formic acid current component to obtain the final background-corrected current-time decay profiles.

3. Results and discussion

3.1. DEVELOPMENT OF PREFERENTIALLY ORIENTED SURFACES

Current-potential profiles of the preferentially oriented (111)- and (100)-Pt surfaces in clean electrolyte are compared to that for a polycrystalline Pt surface in figs. 1A, 1B, and 1C, respectively. Crystallographic modification is easily distinguishable for the (100) surface, but is not as well-defined for the (111) surface, as determined by the degree of peak current development in the hydrogen adsorption-desorption region (-0.20 V to 0.10 V). It must be noted that the voltammetric properties displayed by these oriented surfaces closely approximate those of single crystal Pt surfaces *disordered* by electrochemical sweep into the Pt oxidation region [18,19]. Single crystal surfaces that have been disordered no longer display long-range order, although they exhibit *short-range* order characteristic of the intrinsic crystal orientation [20,21]. These short-range surface order effects are observed in the voltammetry of the obtained preferentially oriented surfaces.

An optical microscope was used for preliminary evaluation of the obtained preferentially oriented surfaces. This technique provided good illumination of the

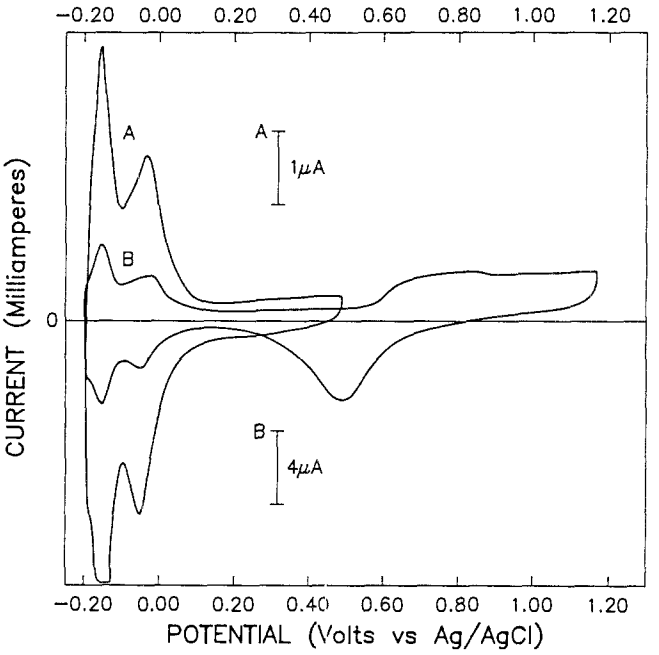

Fig. 1A.

Fig. 1. A: Current-potential profile for (111)-oriented Pt in 0.5 M H_2SO_4; scan rate: 100 mV/s; geometric electrode area: 0.785 mm^2. See text for orientation parameters. B: Current-potential profile for (100)-oriented Pt in 0.5 M H_2SO_4; scan rate: 100 mV/s; geometric electrode area: 0.785 mm^2. C: Current-potential profile for untreated polycrystalline Pt; scan rate; 100 mV/s; geometric electrode area: 0.785 mm^2.

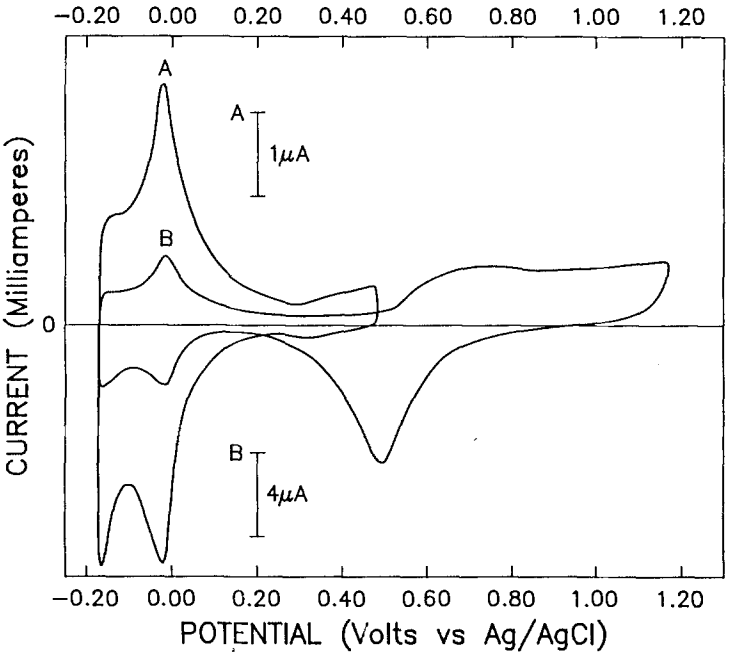

Fig. 1B.

Fig. 1 (continued).

surface, making it easy to distinguish between two contrasting types of grains (ones that were visibly etched or ridged and ones that remained essentially smooth). This type of contrast was not as obvious at similar magnification in the

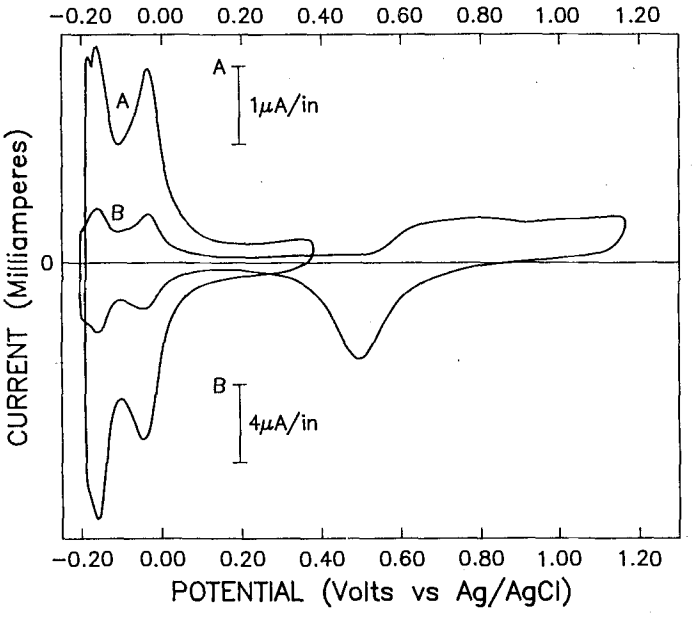

Fig. 1C.

Fig. 1 (continued).

scanning electron micrographs. Visual scrutiny of the number and area of electrochemically etched grains (facets) by optical microscopy (magnification factor $\times 80$) provided semiquantitative evidence for the extent of surface modification (the percentage of the surface with a given preferential orientation) [23]. From this analysis the (111) surface was estimated to be $\sim 60\%$ oriented, while the (100) surface could be estimated at $90 + \%$ (optimally) oriented.

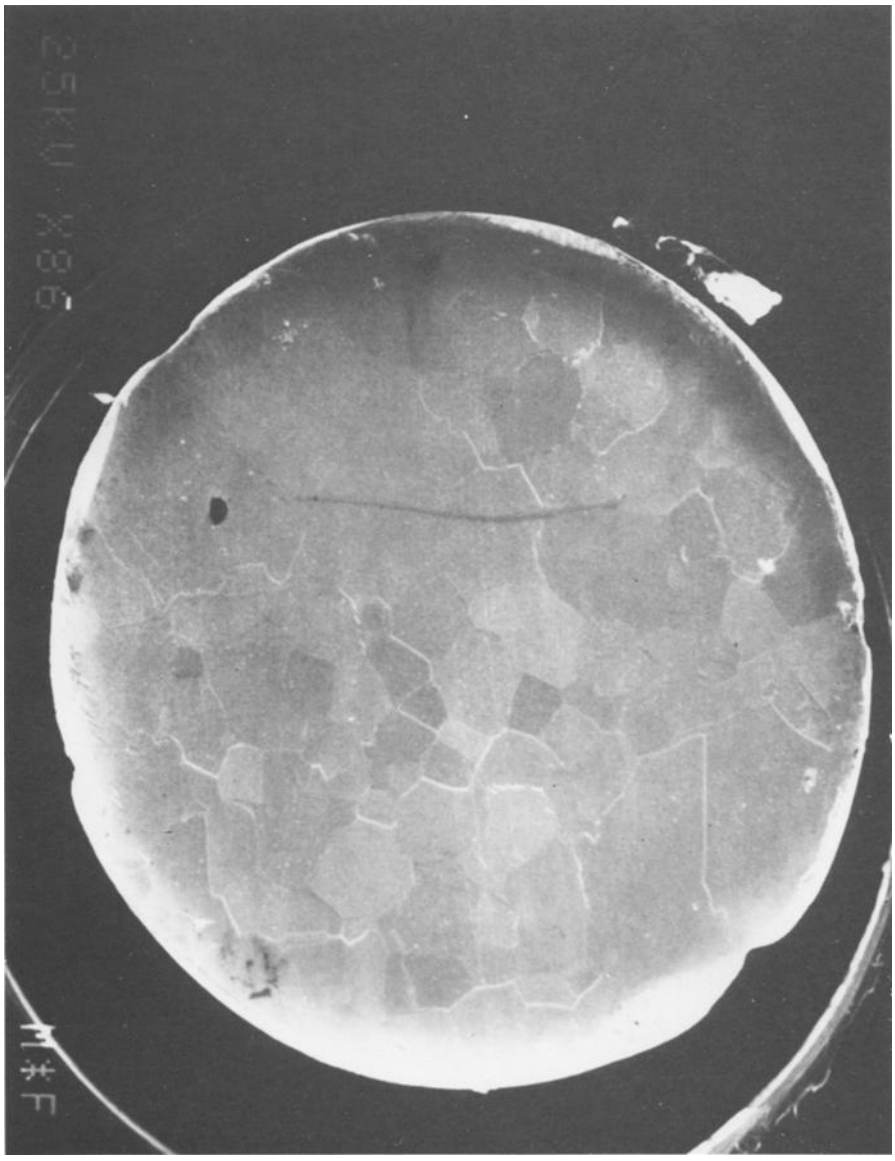

Fig. 2A.

Fig. 2. A: SEM micrograph of (111)-oriented Pt. Magnification factor: $\times 86$. B: SEM micrograph of (111)-oriented Pt. Magnification factor: $\times 400$. C: Electron backscatter pattern. 30 μm spot size.

Assessments of the (111)- and (100)-preferentially oriented surfaces by scanning electron microscopy are depicted in figs. 2 and 3, respectively. (Microscopy of the untreated surface was observed to be essentially featureless: smooth, with diffuse grain boundaries and electron backscatter patterns.) In comparing the micrographs of the modified Pt, surface rearrangement is evidenced by the development of sharp grain boundaries, each grain representing a series of net planes with differing angles of orientation with respect to the substrate plane.

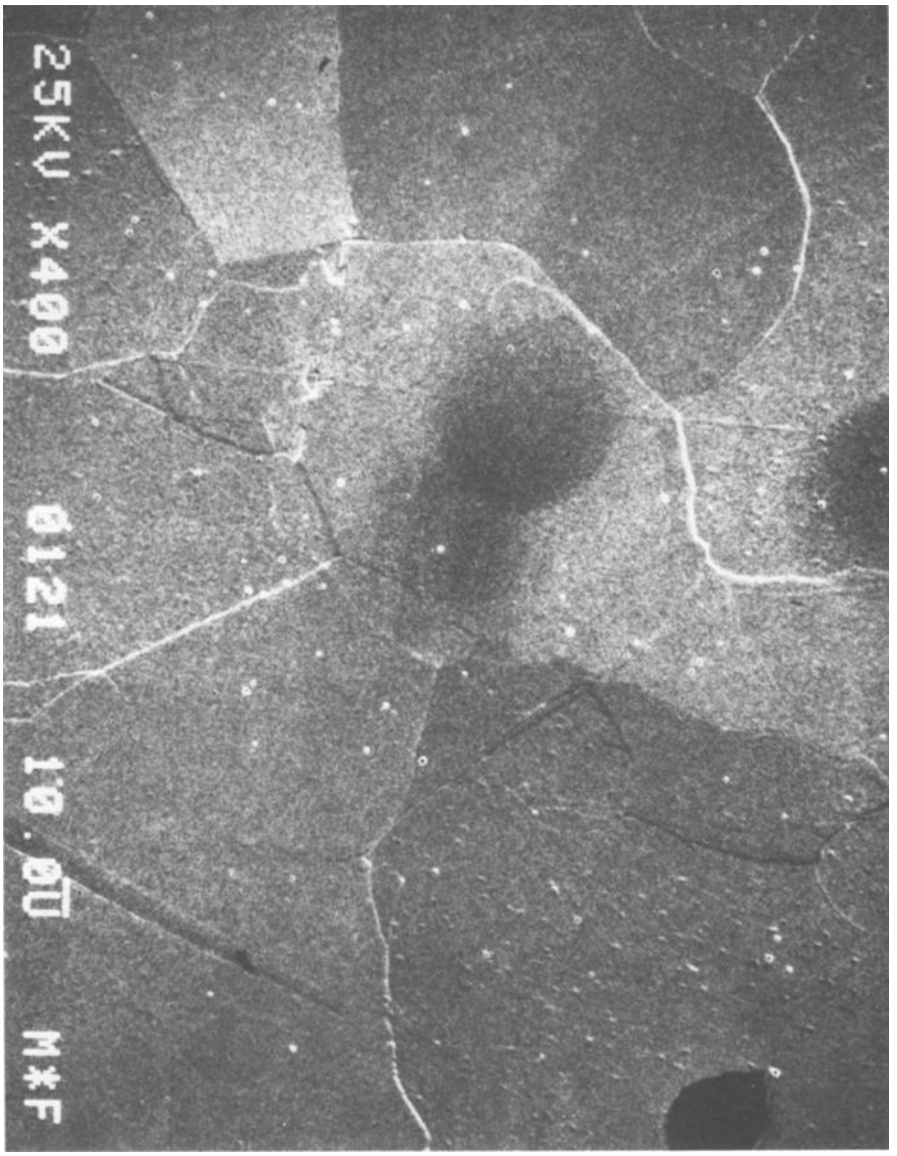

Fig. 2B.

Fig. 2 (continued).

Examination of each surface at low magnification (figs. 2A and 3A) confirmed that the (111) surface was etched to a much lesser extent. Higher magnification analysis of the (100) preferentially oriented surface (fig. 3B) revealed scattered anomalous pyramidal structure formation which can be attributed to (111) orientation development [22]. Reasons for this effect remain to be determined and such structures were observed on fewer than ~ 10% of the grains. However the ridge-like features predominating the bulk of the surface were indicative of

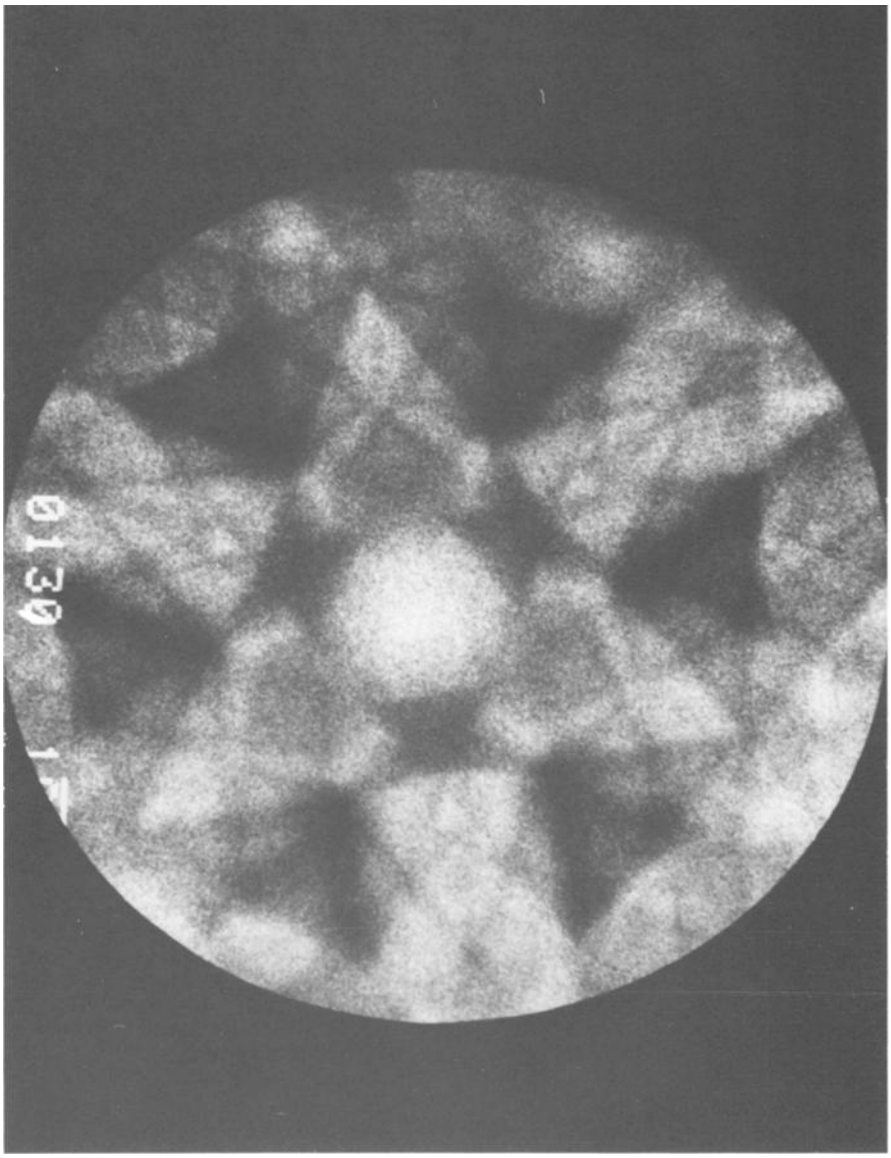

Fig. 2C.

Fig. 2 (continued).

(100) orientation development [22], and clearly depicted in the backscatter pattern (fig. 3C). In the case of the (111) oriented surface the grains reflected little pronounced structure development when compared to the anomalous facets in the (100) surface. This may be due to impurity effects or, more likely, a slower nucleation mechanism for the formation of this surface under the reported conditions. The backscatter pattern of select grains confirmed (111) orientation as evidenced by its characteristic symmetry.

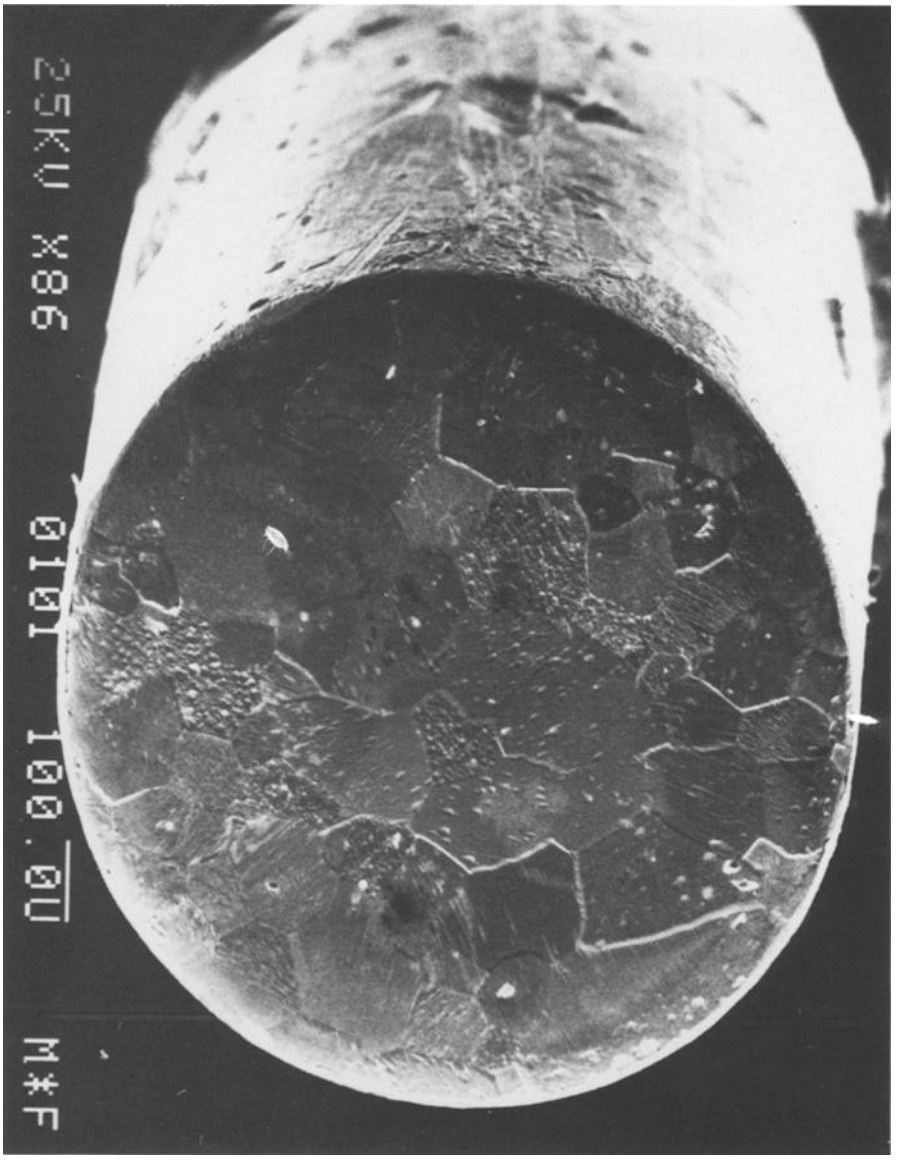

Fig. 3A.

Fig. 3. A: SEM micrograph of (100)-oriented Pt. Magnification factor: ×86. B: SEM micrograph of (100)-oriented Pt. Magnification factor: ×400. C: Electron backscatter pattern. 30 μm spot size.

Electron backscatter patterns can be used to determine crystal orientation in the samples [23]. These patterns can be educed from areas as small as 30 μm in diameter and so it was possible to orient individual grains in these samples. From a study of the orientation of the ridges in the developed regions of the electrode surfaces the electron backscatter patterns (figs. 2C and 3C) reflected the three-fold

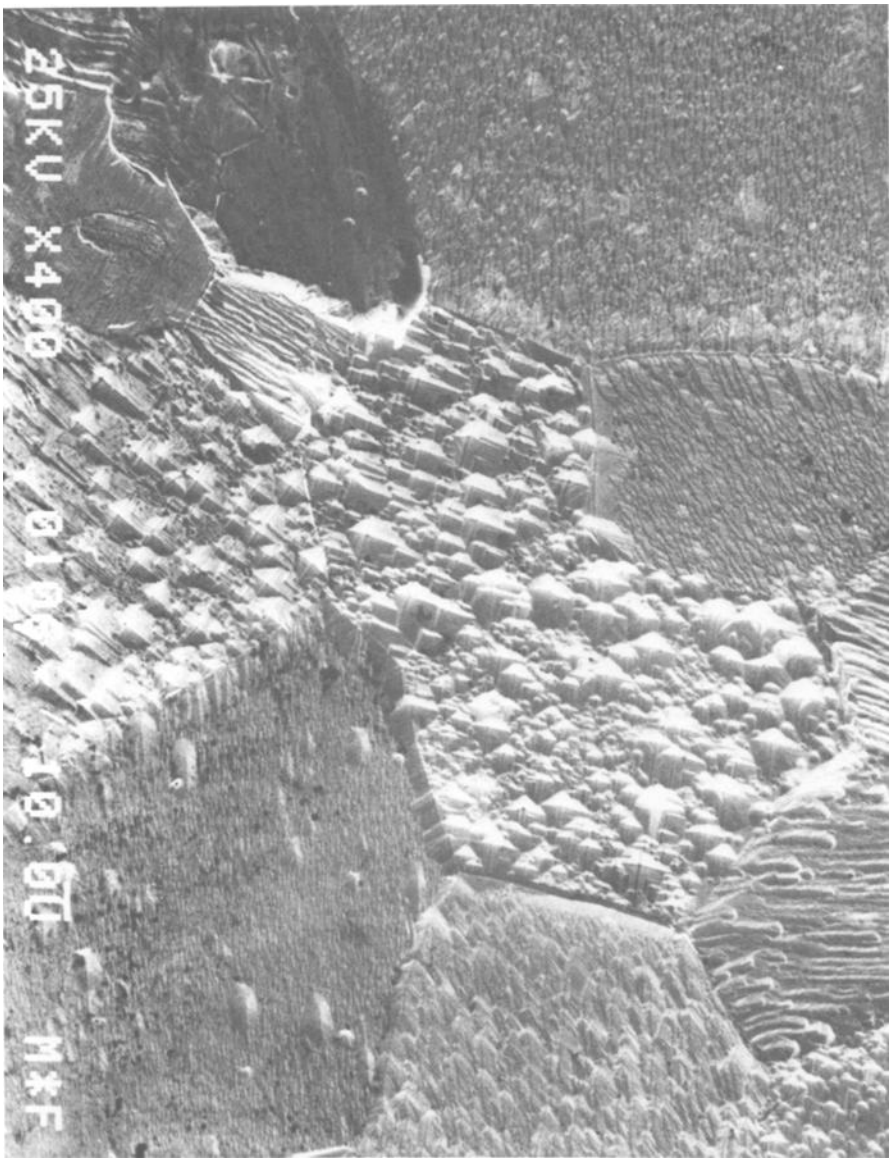

Fig. 3B.

Fig. 3 (continued).

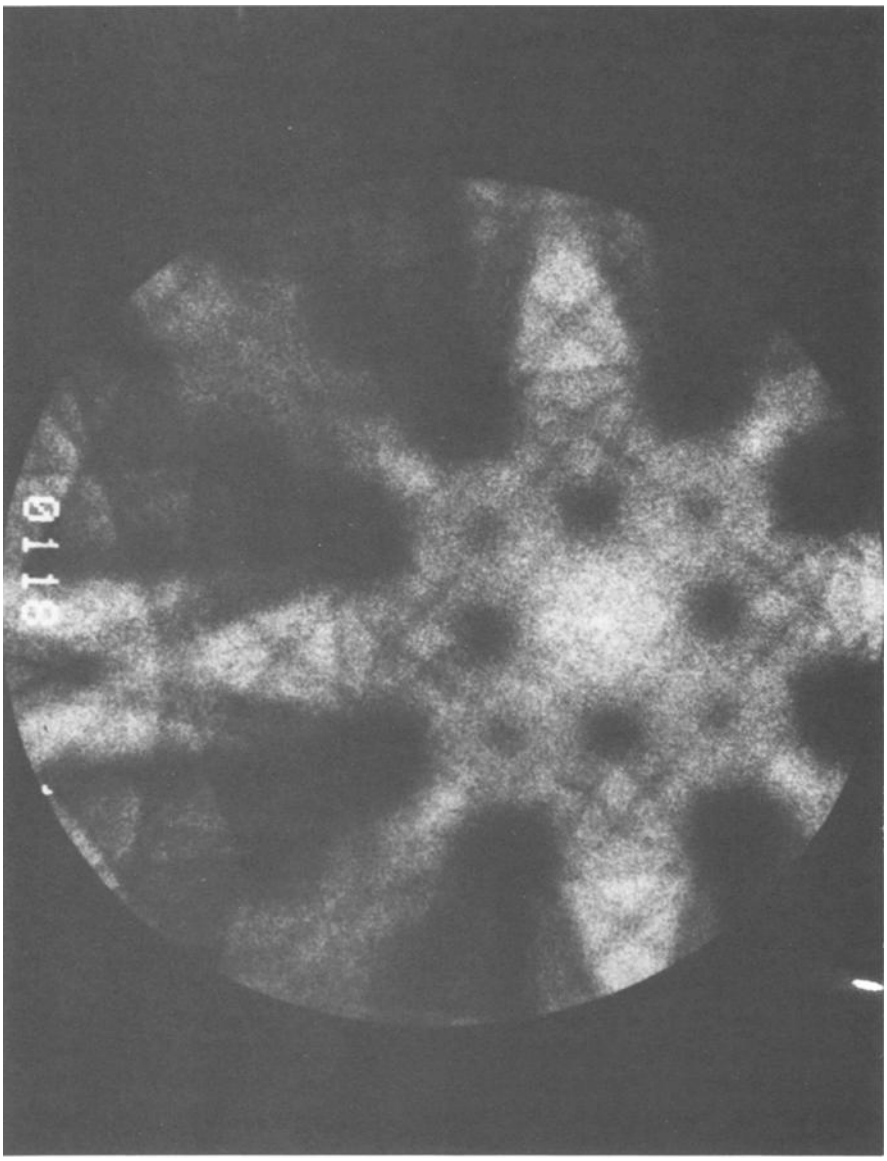

Fig. 3C.

Fig. 3 (continued).

symmetry characteristic of the (111) orientation, with four-fold symmetry observed for the (100) preferentially oriented surface.

3.2. FORMIC ACID: REACTION MECHANISM AND CATALYSIS

Despite some remaining controversy over the exact nature of the HCOOH adsorption mechanism, the dissociative character of adsorption is well-docu-

mented [24–29]. It has been found that the dissociative reaction gives rise to the build-up of a strongly adsorbed intermediate ("poison"). The existence of this poison necessitates a two path mechanism for the overall formic acid oxidation process. The general proposed mechanism [27,28,30,31] follows as:

$$\text{HCOOH} \dashrightarrow \text{COOH} + \text{H}^+ + \text{e}^- \begin{cases} \dashrightarrow \text{poison} \\ \dashrightarrow \text{CO}_2 + \text{H}^+ + \text{e}^-. \end{cases}$$

The poisoning intermediate is oxidized at a peak potential around 0.62 V, that is, just before surface oxidation (on the positive scan) or immediately after reduction of the oxide layer (on the negative going scan). It is the potential range below that for the oxidation of the poisoning intermediate that is of greatest interest in terms of the practical application of these catalysis. The activity of the surface in this range can be assessed by allowing for site competition between the active and poisoning intermediates.

Figures 4 A, B, and C show current-potential profiles for the (111)- and (100)-preferentially oriented Pt surfaces, and polycrystalline Pt, respectively, for the bulk electrooxidation of 0.1 M HCOOH in 0.5 M $HClO_4$. The voltammograms monitor successive sweeps through the lower limit of hydrogen adsorption.

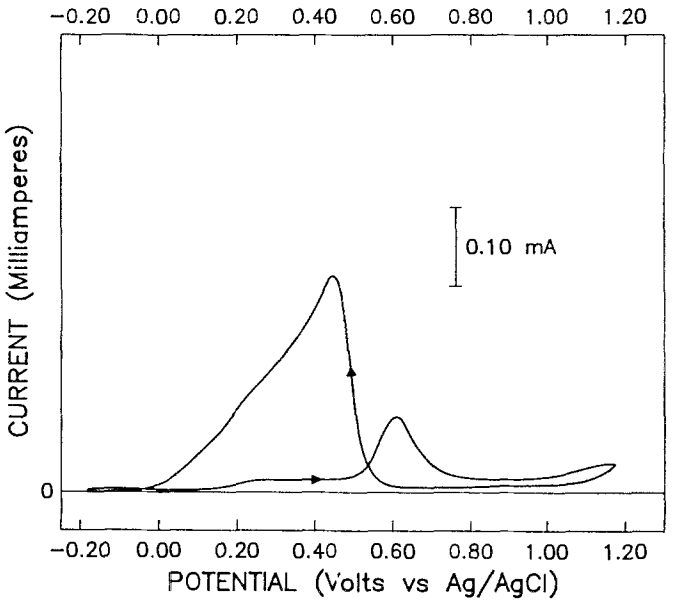

Fig. 4A.

Fig. 4. A: Current-potential profile of formic acid electrooxidation (0.1 M HCOOH in 0.5 M $HClO_4$) on (111)-oriented Pt; scan rate: 100 mV/s; geometric electrode area: 0.785 mm^2. B: Current-potential profile of formic acid electrooxidation (0.1 M HCOOH in 0.5 M $HClO_4$) on (100)-oriented Pt; scan rate: 100 mV/s; geometric electrode area: 0.785 mm^2. C: Current-potential profile of formic acid electrooxidation (0.1 M HCOOH in 0.5 M $HClO_4$) on untreated polycrystalline Pt; scan rate: 100 mV/s; geometric area: 0.785 mm^2.

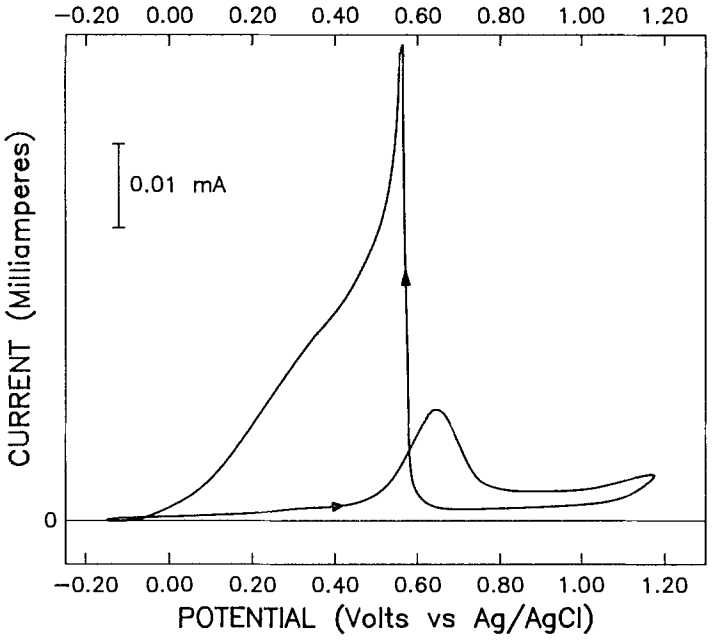

Fig. 4B.

Fig. 4 (continued).

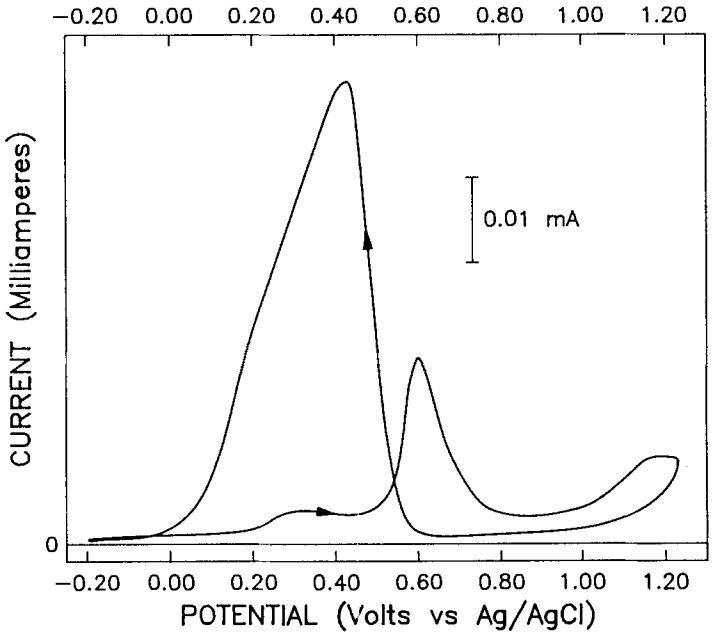

Fig. 4C.

Fig. 4 (continued).

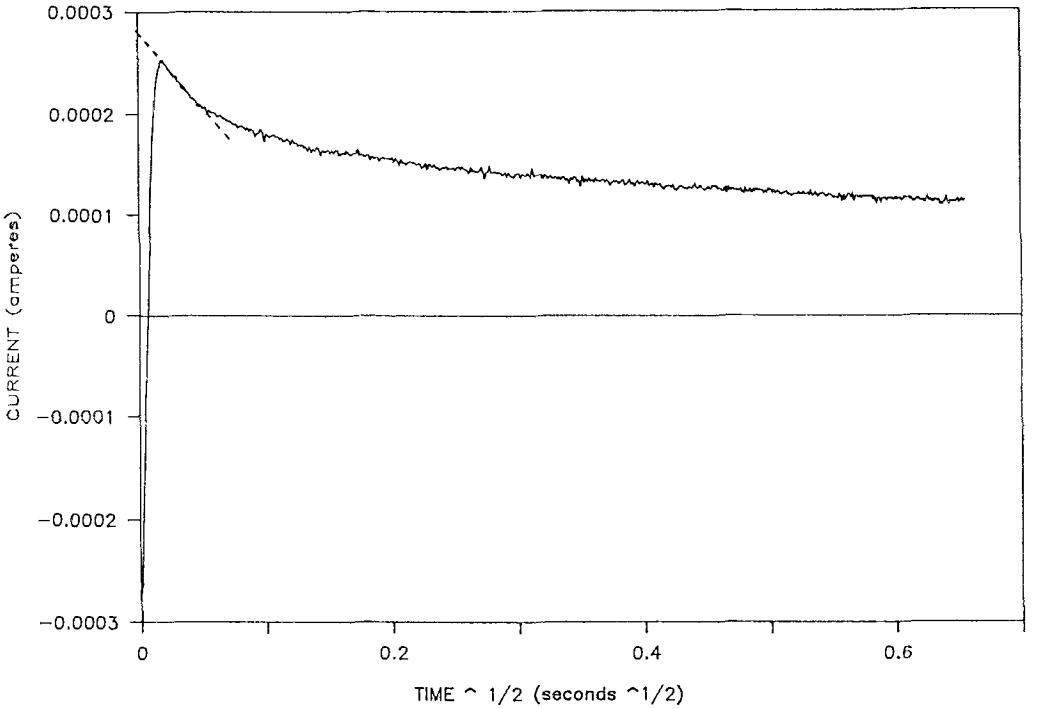

Fig. 5. Current-time response of 0.1 M HCOOH in 0.5 M $HClO_4$ electrolyte, background-subtracted. Potential step: 1.20 V to 0.25 V. Surface: (111)-oriented Pt; geom. area: 0.785 mm^2.

Upon continuous cyclization the observed currents remained constant, indicating no further accumulation of any existing poisoning intermediate. Single crystal studies have shown the ordered Pt(111) orientation to be most highly resistant to poison formation [8,10,11,32,33]. For the case of ordered Pt(111) single crystals, the magnitude of the forward and reverse peak currents are comparable, indicating that the poisoning species has not inhibited oxidation of the active intermediates in the forward sweep. For the case of the disordered preferentially oriented (111)-Pt surface, this effect was not pronounced. This may be explained by the observation that the working surface was not optimally faceted, and remnants of poison-sensitive orientations are diminishing the activity expected in the forward sweep under the applied voltammetric conditions. Alternatively, this contrasting behavior may imply the existence of intrinsic differences between short-range and long-range ordered catalysts. At this time, however, we are unable to delineate these differences.

Figure 5 shows a representative chronoamperometric response of 0.1 M HCOOH in 0.5 M $HClO_4$ at a potential of 0.25 V, for the (111)-oriented surface (the intermediate potential limits to which the electrode was stepped were 0.10 V to 0.45 V in 50 mV increments). This figure serves as an example of the current-time response obtained using the applied potential step program, reflect-

ing mixed diffusion/heterogeneous electron charge transfer control of the oxidative process [34]. Diffusion control is demonstrated by a linear region in the short-time interval, with timescale plotted as $t^{0.5}$. The linear portions of the current-time profiles as shown in fig. 5 were extrapolated back to the current axis, and these current values were used to calculate the reaction turnover rate at each potential for (111)- and (100)-faceted Pt, as well as for polycrystalline Pt, according to the equation:

$$\text{turnover} = i/nFS \times 1/(1.3 \times 10^{15}) \times (6.02 \times 10^{23}),$$

where turnover = rate of oxidation (molec./surface atom-sec), i = extrapolated current (A), n = number of e^- transferred, F = Faraday constant, S = surface area (cm^2), 1.3×10^{15} = number of Pt atoms/cm^2 (shown here for a polycrystalline surface), and 6.02×10^{23} = Avogadro's number.

The real surface area, S, was determined from the hydrogen underpotential deposition desorption charge on the assumption of 210 $\mu C/cm^2$ for the polycrystalline and Pt(100)-faceted substrates, and 230 $\mu C/cm^2$ for the Pt(111)-faceted surface [31]. The number of surface platinum atoms for the faceted surfaces was assumed to be $1.3 \times 10^{15}/cm^2$ and $1.5 \times 10^{15}/cm^2$ for the (100) and (111) orientations, respectively. The total number of sites at the real electrode surfaces were calculated in accordance with the hydrogen underpotential deposition charge. Figure 6 shows a comprehensive plot of turnover rate versus potential for each of the three surfaces. The turnover rates indicate a maximum *fourfold* current enhancement for the (111)-faceted surface versus a polycrystalline surface.

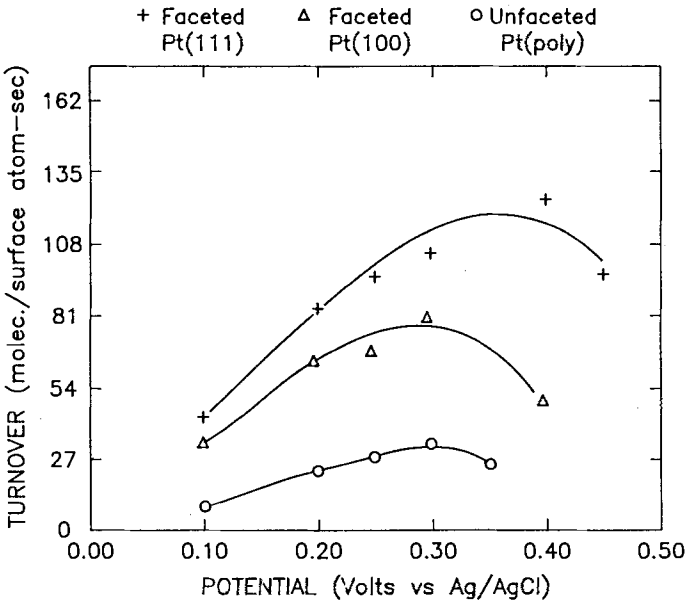

Fig. 6. Plot of HCOOH turnover rate versus potential for untreated polycrystalline, (100)- and (111)-oriented Pt surfaces.

4. Conclusions

The fourfold enhancement in reaction turnover for a (111)-faceted surface is significant and optimistic with respect to the applicability of preferentially oriented surfaces in real-life electrocatalysis, and we emphasize that the turnover results are consistent with those for formic acid electrocatalysis on ordered platinum electrodes [32,33]. These results indicate that the Pt(111) surface is the most highly resistant to poison formation not only when long-range order, but also when *short-range* surface order is produced and preserved upon electrolysis. This is an encouraging results which should activate more research on polycrystalline platinum catalysts modified to display preferential crystallographic specificity, that is, without the need for faceting expensive single crystal materials. The search for catalytically enhancing, crystallographically modified, rough Pt black-type surfaces is particularly challenging in this regard.

Acknowledgements

This work was supported by the Materials Research Laboratory of the University of Illinois via National Science Foundation Grant No. DMR-86-12860. Scanning electron microscopy was carried out in the Center for Microanalysis of Materials, University of Illinois, which is supported by the U.S. Department of Energy under contract DE-AC 02-76ER 01198. We would also like to thank J.B. Woodhouse of the Center for Microanalysis of Materials for his helpful discussions.

References

[1] B.E. Conway, Rev. Pure Appl. Chem. 18 (1968) 105.
[2] B.B. Damaskin, O.A. Petrii and V.V. Batrakov, *Adsorption of Organic Compounds on Electrodes* (Plenum Press, New York, 1971).
[3] A. Capon and R. Parsons, Electroanal. Chem. and Inter. Electrochem. 44 (1973) 239.
[4] A. Capon and R. Parsons, Electroanal. Chem. and Inter. Electrochem. 45 (1973) 205.
[5] A. Wieckowski, in: *Modern Aspects of Electrochemistry*, eds. J. O'M. Bockris, B.E. Conway and R.E. White, No. 17 (Plenum Press, New York) in press.
[6] R. Parsons and T. VanderNoot, J. Electroanal. Chem. 257 (1988) 9.
[7] J. Clavilier, J. Electroanal. Chem. 236 (1987) 87.
[8] R.R. Adzic, A.V. Tripkovic and V.B. Vesovic, J. Electroanal. Chem. 204 (1986) 329.
[9] J. Clavilier and S.G. Sun, J. Electroanal. Chem. 199 (1986) 471.
[10] S. Motoo and N. Furuya, J. Electroanal. Chem. 184 (1985) 303.
[11] C. Lamy, J.M. Leger, J. Clavilier and R. Parsons, J. Electroanal. Chem. 150 (1983) 71.
[12] R.R. Adzic, A.V. Tripkovic and N.M. Markovic, J. Electroanal. Chem. 150 (1983) 79.
[13] J. Clavilier, R. Parsons, R. Durand, C. Lamy and J.M. Leger, J. Electroanal. Chem. 124 (1981) 321.

[14] J.C. Canullo, W.E. Triaca and A.J. Arvia, J. Electroanal. Chem. 175 (1984) 337.
[15] R. Cervino, W.E. Triaca and A.J. Arvia, J. Electrochem. Soc. 132 (1985) 266.
[16] W.E. Triaca, T. Kessler, J.C. Canullo and A.J. Arvia, J. Electrochem. Soc. 134 (5) (1987) 1165.
[17] J.C. Canullo, W.E. Triaca and A.J. Arvia, J. Electrochem. Soc. 200 (1986) 397.
[18] D. Zurawski, L. Rice, M. Hourani and A. Wieckowski, J. Electroanal. Chem. 230 (1987) 221.
[19] L. Palaikis, D. Zurawski, M. Hourani, and A. Wieckowski, Surf. Sci. 199 (1988) 183.
[20] A.T. Hubbard, J. Vac. Sci. Technol. 17 (1980) 49.
[21] F.T. Wagner and P.N. Ross, Jr., J. Electroanal. Chem. 250 (1988) 301.
[22] A.J. Arvia, J.C. Canullo, E. Custidiano, CL. Perdriel and W.E. Triaca, Electrochimica Acta 31(11) (1986) 1359.
[23] Oliver C. Wells, *Scanning Electron Microscopy* (McGraw Hill, New York, 1974) Ch.7.
[24] S.B. Brummer and A.C. Makrides, J. Phys. Chem. 68 (1964) 1448.
[25] M.H. Gottlieb and J. Electrochem. Soc. 111 (1964) 465.
[26] D.R. Rhodes and E.F. Steigelmann, J. Electrochem. Soc. 112 (1965) 16.
[27] A.H. Taylor, R.D. Pearce and S.B. Brumner, Trans. Faraday Soc. 67 (1971) 801.
[28] A. Wieckowski and J. Sobkowski, J. Electroanal. Chem. 63 (1975) 365.
[29] A. Wieckowski, J. Electroanal. Chem. 78 (1977) 229.
[30] Lam-Wing Leung and M.J. Weaver, J. Electroanal. Chem. 240 (1988) 341.
[31] M.W. Breiter, *Electrochemical Processes in Fuel Cells* (Springer-Verlag, New York, 1969).
[32] R.R. Adzic, A.V. Tripkovic and W.E. O'Grady, Nature 296 (1982) 137.
[33] S.G. Sun, J. Clavilier and A. Bewick, J. Electroanal. Chem. 240 (1988) 147.
[34] A.J. Bard and L.R. Faulkner, *Electrochemical Methods* (John Wiley and Sons, New York, 1980).